TRACTION SYSTEM CASE STUDY

L Buhrkall

Consultant, Traction Systems and EMC, Denmark.

The development of a cost-optimal traction system towards a specific set of customer requirements is a complex, iterative process with many pitfalls. The new European market situation, with business-oriented operators specifying only their basic performance requirements and no technical details, and with a multinational industry where components such as motors, inverters, etc. are supplied not only from different departments but from different countries, increases the complexity of the process even further, and with that the risk of sub optimisation. Even in the simplest case, with the only requirement being a maximum run time between two stations with a certain train weight, several very different solutions are all technically possible.

Among the most important (costly!) trade-offs that must be balanced are:

* The number of traction motors vs. the installed traction power;

* Traction motor size, rated power of the 3-phase inverter, and traction motor cooling system;

* Interference requirements and AC and DC line filters;

* DC link voltage, main transformer layout, and line converter design;

* Step-up choppers or direct supply from the DC line

1. NO. OF TRACTION MOTORS VS. MAX. TRACTION POWER

Small metro trains such as London Underground are typically designed as Electrical Multiple Units (EMUs), with distributed traction systems and all axles driven. In the other end of the scale, a typical high-speed train such as the French TGV is designed with a locomotive at each end and a number of intermediate trailing cars, i. e., only a minor number of the axles are driven. On the other hand, the TGV has a much higher power rating and a much higher max. speed than the Underground train. In between these two extremes, lots of different designs are seen: 4-car EMUs with 50 % of the axles driven (e. g., Class 465), and many more.

Figure 1. London Underground Bakerloo Line EMU.
Photo: Ross Aitken (aos@cableinet.co.uk) [12]

Figure 2. SNCF TGV Atlantique # 325 (holder of the world speed record, 515.3 km/h). Photo by Didier Egiole (egiole_d@epita.fr) [12]

It is quite obvious even to a non-expert that the TGV is superior to the Underground train when it comes to moving people from Paris to Lyon within a given timeframe. It might be more surprising, but nonetheless true, that the Underground train also performs its duties far more efficient than a TGV would do, provided it could be shrunk to fit the narrow loading gauge of the Tube.

This leads to an interesting question: When are a high number of small motors superior to a few high-power ones, and vice-versa? All taken more general: What is the cost-optimal solution with respect to a) the number of driven axles and b) the installed power in the train, if a given set of performance requirements (such as run time over a certain route) must be met?

This problem will be analysed by designing a traction system against the following very basic performance specification:

Performance Specification

* The route is a single 5 km long line with an uphill gradient of G = 10 ‰ between km 1 and km 3, while the rest of the track is horizontal.

* The train must run this 5 km distance in 4 min or less, from start to stop.

* The train is designed as a conventional 4-car EMU, with 2 2-axle bogies per car.

* The estimated train weight at max. load is m = 170 t. The axle load of non-driven axles is 10 t, while the remaining weight is distributed evenly on the motorised axles.

* A maximum value of the wheel-to-rail friction coefficient μ = 15 % must be taken into account in the performance calculations, in order to make sure that the timetable can be met also at wet rail conditions.

* No other performance requirements or customer preferences (such as redundancy, Life Cycle Cost, or whatever) are considered.

Already at this point it is clear that the design process must be iterative with several loops, and that "guesstimates" must be made at several levels. There is no way a traction system can be designed without knowledge about the total weight of the train, but this weight is not known until the traction system has been designed. The weight of similar already existing trains can give a starting point, but be careful - train weights are often underestimated at the beginning of a new project.

It is also clear that the given performance specification is very basic. In practice, specifications that simple are only seen in the special case of dedicated Airport Express Shuttle Trains. In the general EMU specification, minimum run times are specified for a number of longer routes each with several station stops, and special requirements concern the emergency operation in case parts of the traction system are cut-out due to faults.
A typical locomotive specification requires that a certain train weight must be accelerated from stand still on a certain uphill gradient, and the track must be cleared within a certain minimum time. Additional technical requirements could be anything from line current or line power limitations down to customer preferences for certain types of power semiconductors.

Altogether this means that the typical performance simulation will be much more comprehensive than the one given in the example below which should be seen as an illustration of the basic principles only.

Over and above this, the changing market situation means that questions like Total Cost of Ownership, flexibility (it must be possible to lease out a given vehicle to many different operators), and reliability (the operator has a contractual obligation that say 99 % of the trains must be on time) are becoming increasingly important. Typically, such considerations lead to an increased number of iteration loops in the traction system design process.

Tractive effort (TE) diagram. Generally, 3 factors limit the tractive effort vs. speed F(v) (figure 3):

* Max. tractive effort F_{MAX}

* Max. speed v_{MAX}

* Max. power P_{MAX}, giving $F(v) = P_{MAX}/v$ {1}

(A 4th potentially limiting factor, the pullout torque of the asynchronous motor, will be treated in section 2.)

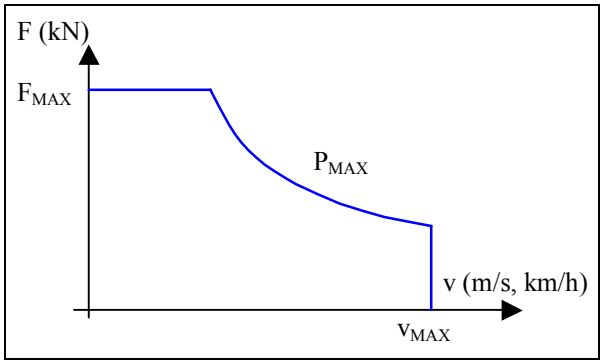

Figure 3. Generic tractive effort (TE) diagram.

The maximum tractive effort that can be transferred to the rail and thus utilised for acceleration is limited by the total axle load of the motorised axles m_m and by the friction coefficient μ:

$$F_{MAX} \leq \mu \cdot m_m \cdot g \qquad \{2\}$$

With 4, 6, or 8 motorised axles and the specified weight distribution, {1} leads to:

No. of motors	Total axle load, motorised axles	Maximum tractive effort
n	$m_m = 170-(16-n)\cdot 10$	$F_{MAX} = \mu \cdot m_m \cdot g$
4	50 t	73.6 kN
6	70 t	103 kN
8	90 t	132 kN

Table 1. Maximum TE vs. number of motors.

In the actual case, P_{MAX} and v_{MAX} are outputs from the performance simulation, see below.

Running resistance. The running resistance is due to static friction, dynamic friction, and aerodynamic resistance. Numerous formulas have been suggested; here the simple one from [1] is used:

$$F_R(v) = 10^{-3}\cdot(2.5 + 10^{-3}\cdot k\cdot(v+\Delta v)^2)\cdot m\cdot g \qquad \{3\}$$

where $k \approx 0.33$ for normal passenger trains and $\Delta v \approx 15$ km/h accounts for the wind speed. It should be noted however that many other formulas such as Davies include a linear (i. e., proportional to v) term.

Gradient force. The gradient force is calculated as

$$F_G(s) \approx m\cdot g\cdot G(s)/1000 \qquad \{4\}$$

which is an acceptable approximation for all normal gradients G < 100 ‰. The route profile of the actual example with the 10 ‰ gradient is shown in figure 4.

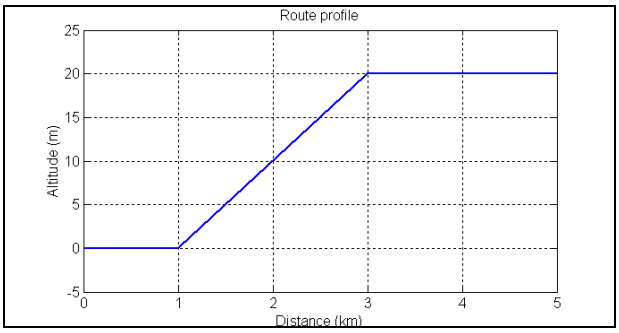

Figure 4. Route profile.

Performance simulation. A simple performance simulation program could have the following structure:

1. Define a tractive effort vs. speed curve F(v) based on F_{MAX}, and (in the actual case) guessed values of P_{MAX} and v_{MAX} (in other cases, these figures might already be fixed). Define a similar curve B(v) for braking.

2. Calculate a vector with train speed vs. distance by means of a discrete integration. The generic formula $v^2 - v_0^2 = 2as$ leads to:

$$v(s) = \sqrt{2\cdot\frac{F(v(s-\Delta s)) - F_R(v(s-\Delta s)) - F_G(s)}{m_{DYN}}\cdot\Delta s + (v(s-\Delta s))^2}$$

however, *v(s)* must be limited to v_{MAX}. Select Δs small enough to avoid numerical problems, e. g., Δs = 1 m. m_{DYN} is the "dynamic mass" of the train, i. e., including the rotating masses. Typically, $m_{DYN} \approx 1.15\cdot m$.

3. Repeat 2., but running backwards on the route from s = s_{MAX} with B(v) instead of F(v), and with negative values of F_R and F_G. Compare the two v(s) vectors, and select the smallest values.

4. Calculate a time vector t(s):

$$t(s) = t(s-\Delta s) + \frac{2\cdot\Delta s}{v(s)+v(s-\Delta s)}$$

5. Repeat - if necessary - with new P_{MAX} and/or v_{MAX} values until the run time is as specified.

Simulation results. The figures 5 and 6 can be made by means of the above procedure and a few lines of Matlab code. B(v) has been assumed to be equal to -F(v).

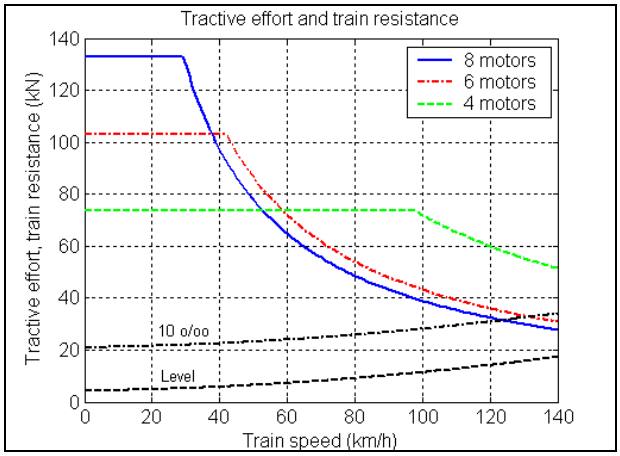

Figure 5. Tractive effort curves.

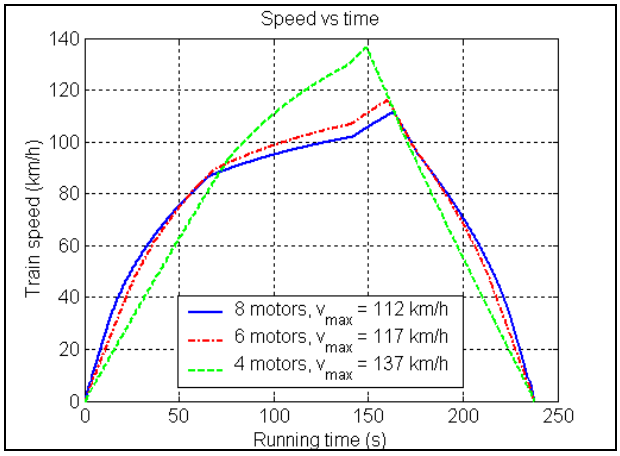

Figure 6. Train speed vs. time.

The following combinations of number of traction motors and P_{MAX} and v_{MAX} meet the run time requirement of 4 min. (240 s):

No. of motors	v_{MAX}	P_{MAX}
4	137 km/h	2.0 MW
6	117 km/h	1.2 MW
8	112km/h	1.08 MW

Table 2. Specification compliant traction systems

Energy Consumption. In addition to the installed power, the energy consumption is traditionally an important parameter when comparing different designs.

The fundamental relationships $P = F \cdot v$ and $W = \int P\, dt$ lead to the curves in figure 7. The losses of the overall traction system have been assumed to be 15 % of the rail power. In a detailed simulation, more accurate models of the traction motor and other systems should be used, cf. section 2.

The higher power and the higher top speed with 4 motors lead to a 20-30 % increase of the energy consumption, compared to the other alternatives.

The regenerative braking (100 % regeneration has been assumed) feeds approximately 1/3 of the gross energy back to the supply system.

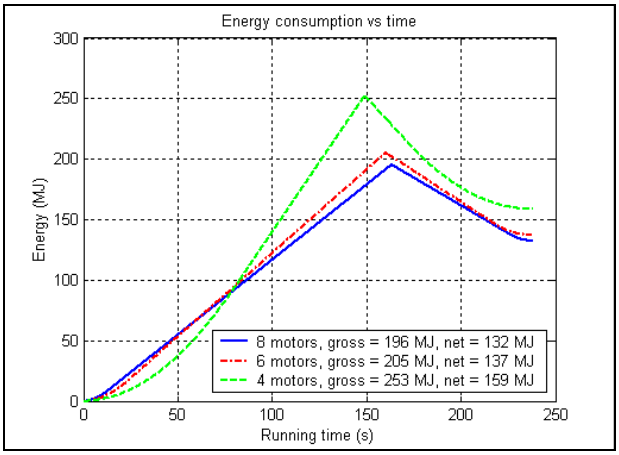

Figure 7. Energy consumption.

Discussion. It seems quite clear - provided no other factors are considered - that the 8 motor solution is less attractive compared to 6 motors. It is unlikely that the marginal savings in speed, power, and energy consumption can balance the cost of another 2 motors and drive systems, except maybe at certain special conditions.

The choice between 4 and 6 motors is less evident. It is possible that a definite answer can only be given if both designs are completed in parallel, and the total costs are evaluated. So in order to continue, a shortcut is made:

Specification addendum # 1

* A design with 3 independent traction systems provides better performance in case one system fails.

* The lower peak power of the 6 motor solution is favourable from a power supply point of view.

* In any case, the speed limit of the line is 120 km/h.

* The wheel diameter and gear ratio are such that a motor speed of 4500 r/min corresponds to 120 km/h.

2. TRACTION MOTOR SIZE VS INVERTER SIZE

Max. motor torque. The torque of the asynchronous motor is given by the equation

$$T = k_1 \cdot V_{ROTOR} \cdot J \cdot B \cdot \cos(\phi_i) \qquad \{5\}$$

where V_{ROTOR} is the active volume of the rotor, J is the stator surface current density, B is the air gap flux density, ϕ_i is the angle between the J and B vectors, and k_1 is a constant which depends on the winding details, number of poles, etc. [2].

As the maximum flux density is limited due to the magnetic saturation of the iron, {5} shows that in principle we have 2 ways of getting more torque:

* Take a physically bigger motor (increase V_{ROTOR})

* Increase the current density J

However, $\cos(\phi_i)$ decreases if the torque level is increased by means of more current. This leads to the characteristic relationship between torque and slip of the asynchronous motor (figure 8), with the pullout torque limitation. I. e., it is useless to increase J in excess of the limit given by the pullout torque.

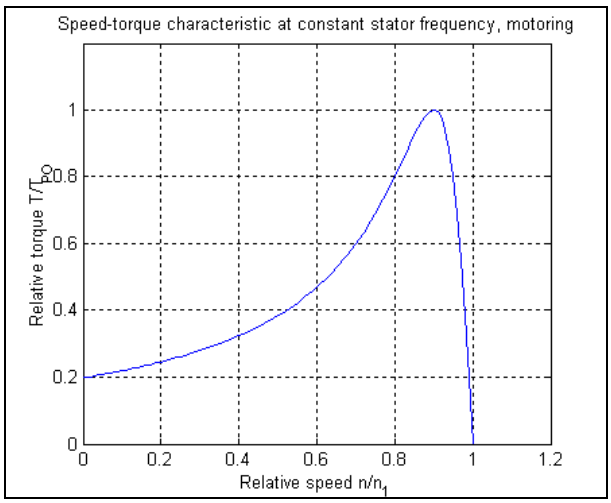

Figure 8. Speed-torque characteristic

The pullout torque of a given motor is a function of voltage and speed, approximated by

$$T_{PO} = \frac{k_2}{L_\sigma} \cdot \left(\frac{U_1}{f_1} \right)^2 \qquad \{6\}$$

where U_1 and f_1 are stator voltage and frequency, L_σ is the leakage inductance, and k_2 is a constant [3]. As the train speed is proportional to f_1 (except for a small slip), {6} shows that the pullout torque will decrease rapidly at high speeds where the 3-phase voltage cannot be increased in proportion to the frequency. This is one of

the fundamental limitations of a 3-phase inverter drive supplied from a basically constant DC link voltage.

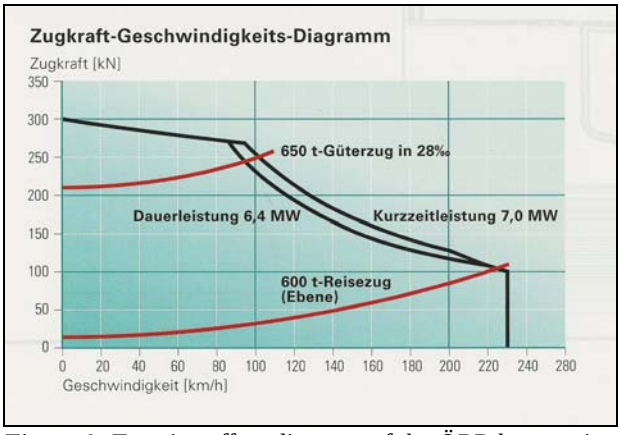

Figure 9. Tractive effort diagram of the ÖBB locomotive class 1116. Notice the reduction of the short time power (Kurzzeitleistung) at high speeds, due to pullout torque limitations. Diagram courtesy Siemens.

Torque and Power. The required motor torque vs. speed T(v) is calculated from the F(v) characteristic based on power balance:

$$T(v) = \frac{F(v)\cdot v}{\eta_{GEAR}\cdot\omega} = \frac{F(v)\cdot v}{\eta_{GEAR}\cdot 2\pi n/60} \qquad \{7\}$$

Expressed in %, the gearbox efficiency η_{GEAR} can typically be assumed to be (100 - no. of gear stages), i. e., 99 % if a 1-stage gearbox is used.

{8} below gives the required electrical power from the inverter, which is calculated from the TE (and BE for braking) diagram as

$$P_{INV}(v) = \frac{F(v)}{v\cdot\eta} \qquad \{8\}$$

where the efficiency η of the traction motor is assumed to be 0.9 in the following calculations. In more exact calculations, {8} should be replaced by a proper motor model.

Provided the voltage characteristic of the inverter is known, the required current supplied from the inverter can be found as

$$I_{INV}(v) = \frac{P_{INV}(v)}{\sqrt{3}\cdot U_{INV}(v)\cdot\cos(\varphi)} \qquad \{9\}$$

where cos(φ) in these simplified calculations is assumed to be 0.85. (Normally cos(φ) will vary with speed and load. Again, a more detailed model should be developed).

2 different designs. Suppose the train is being designed to run directly on a 750 V DC supply. This means that the maximum phase-to-phase voltage fundamental at the inverter output is

$$U_{INV,MAX} = 750\cdot\frac{4}{\pi}\cdot\cos\left(\frac{\pi}{3}\right) = 0.78\cdot 750 = 624\,V \qquad \{10\}$$

This comes from the Fourier series of the phase-to-phase voltage wave shape in figure 10.

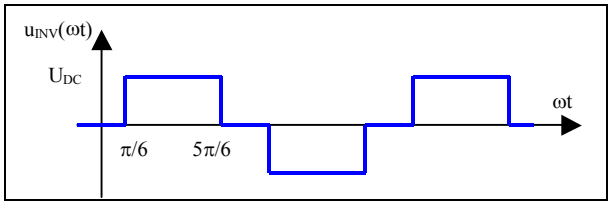

Figure 10. Wave shape at max. inverter output voltage

Now let the inverter output voltage hit its maximum value at 42 km/h and at 70 km/h, respectively. Below these so-called base speeds, voltage is kept proportional to frequency (i. e., the flux is constant) by means of Pulse Width Modulation (PWM).

The details of the corresponding motor designs (number of windings, etc.) are optimised to each of these strategies. It is normally possible (within certain limits) to adapt a given motor to another voltage vs. frequency characteristic by rewinding the stator. An increased base speed requires fewer winding turns but a thicker wire.

The figures 11 and 12 show the characteristics of these two options. It should be noticed that the torque curves T(v) are equal in the two figures.

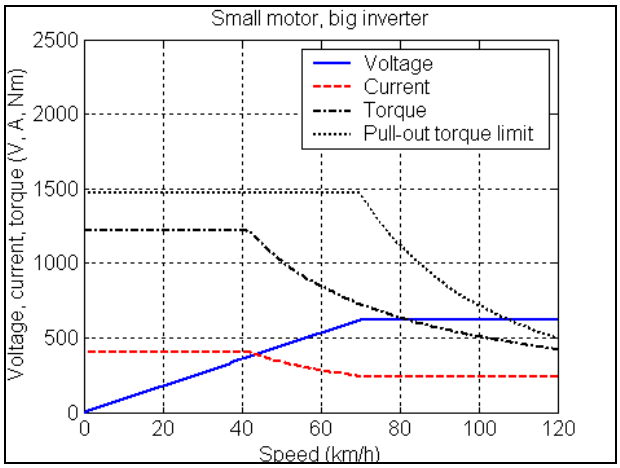

Figure 11. Small motor, big inverter

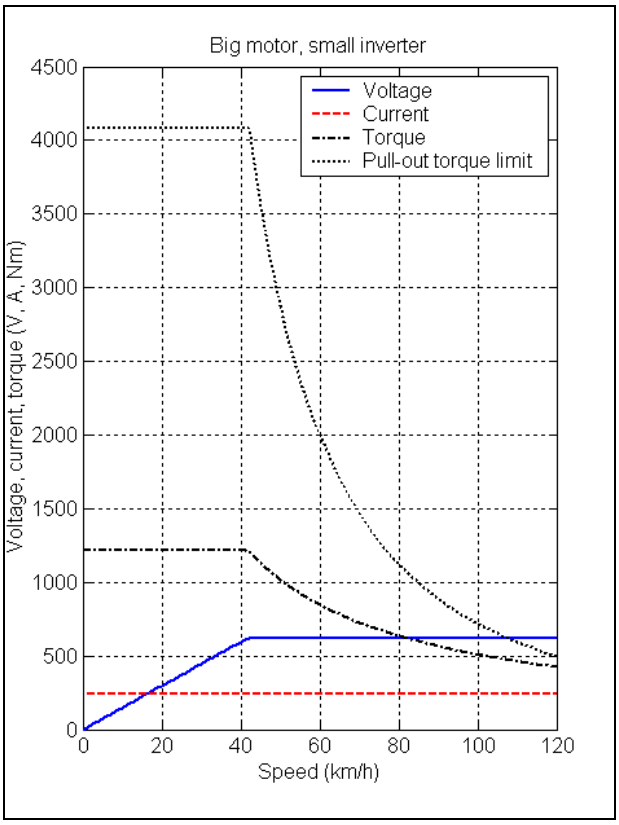

Figure 12. Big motor, small inverter

Discussion. The motor in figure 12 operates in the field weakening range (i. e., at constant 3-phase voltage (figure 10), meaning that the U_1/f_1 ratio decreases with increasing frequency) for almost 2/3 of the entire speed range. In order to compensate for the low air gap flux density at max. speed, {5} gives that the rotor volume and thus the entire motor must be big.

In figure 11, the motor size is more optimal. The field weakening range is smaller, meaning that the relative air gap flux density is higher at max. speed. This allows the motor to be much smaller than the one in figure 12, and the pullout torque is just slightly higher than the actual torque in most of the speed range.

The penalty is an oversized inverter. The semiconductor ratings are basically determined by the maximum current and the DC link voltage. The 70 % higher current at low speed necessitates an inverter with a higher kVA rating, even though the rated power of the total system has not increased.

The systems can be summarised as follows:

	Rel. motor size	Rel. inverter size
Figure 11	*1*	*1.7*
Figure 12	*2.8*	*1*

Table 3. Comparison of system designs

It must be stressed that the given performance requirements can not be met by combining the small inverter of figure 12 with the small motor of figure 11.

The system of figure 12 was generally recommended in the early days of asynchronous traction (e. g., [4]), but the development of cheaper and more efficient semiconductors such as IGBT's has made it possible to increase the power of a single normal-gauge traction motor to 1.6 MW [5], thus moving the trend towards figure 11.

Figure 13. 6.4 MW locomotive (1.6 MW per traction motor), ÖBB class 1116, cf. figure 9. Photo by István Halász (hihihihi@freemail.hu) [12]

Thermal considerations. The higher current at low speeds means that the total RMS current during a run is 20 % higher with the smaller motor than with the bigger one (figure 14).

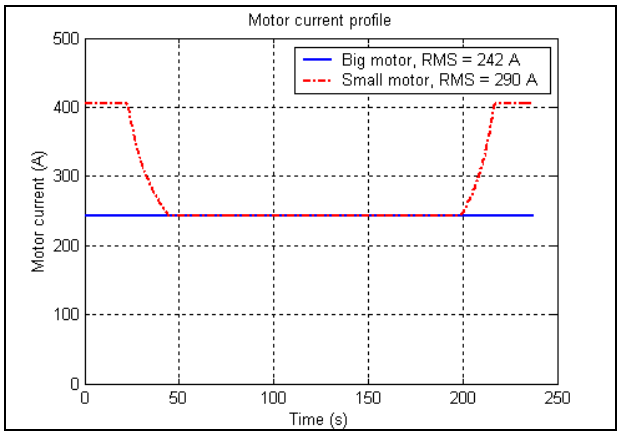

Figure 14. Motor current profile.

It is clear that the cooling of the heavier loaded but physically smaller motor must be designed with higher capacity in comparison with that of the bigger motor. 4 main types of traction motor cooling arrangements exist:

* Self-cooling, encapsulated motor with an axial fan

* Self-cooling, open motor with an axial fan

* Forced air cooling with an external fan

* Water-cooling

The cost of the cooling equipment is an important factor when choosing between different traction system layouts. If, as an example, the small motor of figure 11 requires forced air cooling, meaning that fans, ducts, filters, etc., must be installed in the carbody, while the bigger motor of figure 12 can be totally encapsulated and self-cooled like an industrial motor, then that is an important argument in favour of the big motor - small inverter solution.

3. DC-AC TRACTION SYSTEMS: LINE INTERFERENCE CURRENTS AND DC LINE FILTER DESIGN

System layout. The majority of DC-AC traction systems (i. e., systems with supply from a DC electrified 3rd rail or overhead line and with 3-phase AC traction motors) are equipped with 3-phase inverters that are basically designed to operate directly at the supply voltage, only protected by the High Speed Circuit Breaker and the line filter.

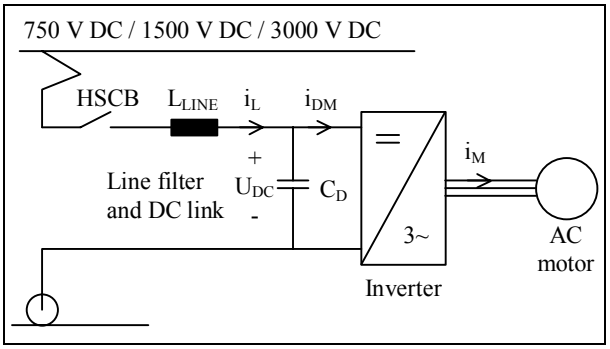

Figure 15. DC traction system

One of the important issues when designing such a system is line interference. The 3-phase inverter converts the basically constant DC link voltage into a 3-phase AC voltage with variable amplitude and variable frequency. The 3-phase voltage however is not sinusoidal, and consequently, the currents at both the DC side (i_{DM}) and the AC side (i_M) of the inverter have rather high contents of current harmonics. The current harmonics at the DC side are generally undesirable because they have the potential of interfering with signalling and communication systems. The line filter attenuates these currents, but as passive filter components are heavy and bulky it is important to consider the problems of line interference already when selecting the motor/inverter combination, and when designing the control systems for the 3-phase inverter.

Stator flux vector. The trajectory of the stator flux vector of the 3-phase motor provides an informative illustration of the origin of the current harmonics and as such, it is a helpful tool for qualitative analysis.

In-depth information about the concept of flux control can be found in several books and papers (e. g., [6] and [7]). For the purpose of the present analysis, however, it is only necessary to recognize that the stator flux vector ψ of an AC motor supplied from an ideal 3-phase sinusoidal voltage source (e. g., the 3x400 V AC mains) rotates with constant angular velocity ω on a circular trajectory that is symmetrically located in the α-β plane, according to figure 16 below.

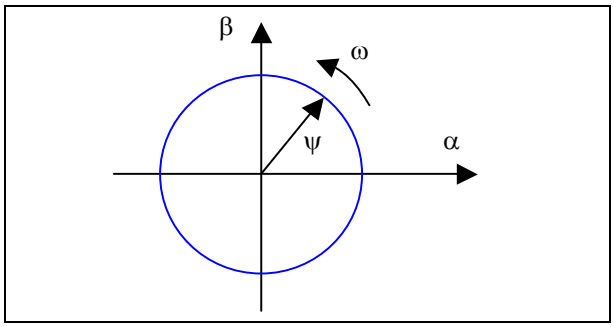

Figure 16. Stator flux trajectory, sinusoidal voltage

Regular current harmonics. Any deviation from the ideal conditions of a circular flux trajectory leads to generation of current harmonics. The greater the deviation, the higher the levels. As an example, take the square wave voltage of figure 10. This voltage generates a hexagon stator flux trajectory.

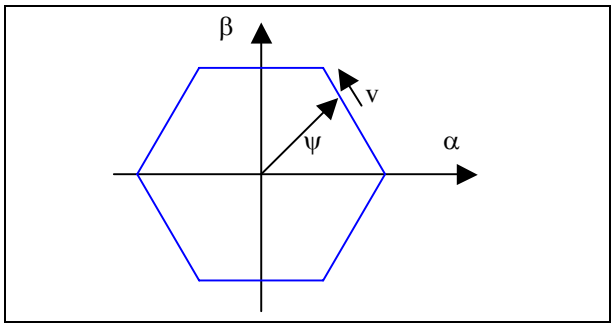

Figure 17. Hexagon flux trajectory

The hexagon trajectory deviates from the ideal circle in two ways:

* The amplitude of the stator flux (length of the vector) varies - the amplitude is higher in the corners of the hexagon

* The vector moves with a constant speed along the perimeter of the hexagon. This means that the angular speed is not constant - it is lower in the corners.

The fact that these deviations are repeated 6 times during each complete revolution of the flux vector means that current harmonics with frequencies of 6, 12,

18, . . . times the actual stator frequency are found at the DC side of the inverter (i. e., as components in i_{DM}) when it operates at the given conditions with maximum output voltage, i. e., throughout the field weakening range.

Specification addendum # 2

* Both of the motor/inverter combinations described in section 2 utilise a 4-pole traction motor (n_{PP} = number of pole pairs = 2).

Reed track circuit interference. The previously specified gear ratio / wheel diameter combination (120 km/h ≈ 4500 r/min) and the base speeds of 42 km/h and 70 km/h, respectively, lead to the following where the base frequency f_B (i. e., the stator frequency at the base speed v_B) is calculated as $f_B = \frac{4500 \cdot v_B \cdot n_{PP}}{120 \cdot 60}$:

Inverter/motor combination	Base speed v_B	Base frequency f_B	$6 \cdot f_B$
Big motor/ small inverter	42 km/h	52.5 Hz	315 Hz
Small motor/ big inverter	70 km/h	87.5 Hz	525 Hz

Table 4. Base frequencies and 6th harmonics

The reed track circuits commonly used in the UK operate at a number of frequencies in the band from 363 Hz to 423 Hz. This means that the 6th harmonic of the big motor / small inverter combination will sweep right across the reed frequency band during every acceleration. This will put severe requirements on the line filter, and probably lead to an overall heavy solution.

The base frequency of small motor / big inverter combination on the other hand is so high that its 6th harmonic is located way above the critical frequency band. The sweep of $6 \cdot f_S$ through the reed frequencies takes place below f_B, where the level of the 6th harmonic can be significantly reduced by means of pulse pattern optimisation.

Current harmonics below base speed. In terms of the stator flux vector, operation below base speed (i. e., with reduced inverter output voltage and constant U/f ratio) is characterised by the introduction of stop points along the perimeter of the stator flux trajectory. By stopping the flux vector on a regular basis, the average rotational speed becomes lower (reduced stator frequency), and as the stop points correspond to zero voltage, the average voltage is reduced too.

Numerous strategies have been proposed for this mode of operation, and it is quite common that different methods are used throughout the speed range from stand still to base speed:

* The flux trajectory can be hexagon shaped like in figure 17, or a more circular shape can be aimed for, e. g., by locating all stop points equidistant along the perimeter of a circle

* The switching frequency of the 3-phase inverter can be synchronised to the stator frequency, or it can vary independently or be constant

* The switching pattern (i. e., the shape of the flux trajectory and the location of the stops) can be predetermined at any stator frequency, or it can be the result of an on-line calculation (e. g., by hysteresis control or similar)

The choice between one or another strategy depends on a number of factors such as the maximum switching frequency of the inverter (determined by the power level and the type of semiconductors used), the interference requirements, and last but not least by tradition and by the emotional feelings of the engineers who design the inverter control system.

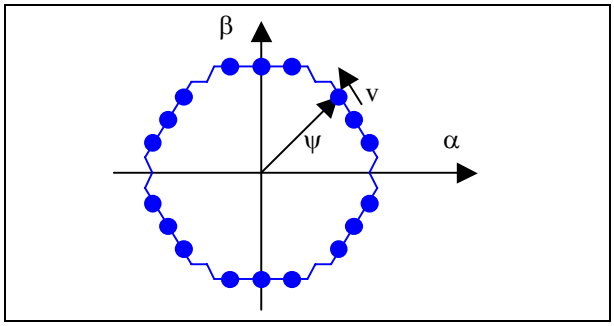

Figure 18. Flux trajectory with corner folding and stops

Figure 18 shows an example of a flux trajectory that has been modified to become more circular by means of so-called corner folding, and with a number of stops along the perimeter. In this case, the current harmonics at the DC side of the inverter are located at the following frequencies:

* The stop frequency f_{STOP} and its multiples, where $f_{STOP} = 3f_{SW} - 9f_S$, ($f_{SW}$ is the switching frequency and f_S the stator frequency)

* 6, 12, 18, . . . times f_S, due to the shape of the flux polygon. The corner folding provides a significant reduction (but not a complete cancellation!) of the level of the 6th harmonic compared to the hexagon shape of figure 17

* Intermodulation products between the above

As another example, the DC-side current harmonics caused by the sine modulation strategy are located at the frequencies $f_H = n \cdot f_{SW} \pm ((3/2) \cdot (1-(-1)^n) + 6 \cdot k) \cdot f_S$, where n = 1, 2, 3, . . . and k = 0, 1, 2, . . .

Irregular harmonics. The term irregular harmonics is commonly used to characterise the additional DC side current harmonics that are caused by power circuit asymmetries, component tolerances (e. g., variations in switching characteristics, time delays, and voltage drops of the power semiconductors), and other imperfections. Typically, such irregularities lead to the generation of a DC component in the 3-phase motor currents, a condition that in turn causes the stator frequency f_S to be present in the DC side current components.

In terms of stator flux, this condition (DC in the motor currents) corresponds to an asymmetrical location of the flux trajectory in the α-β plane.

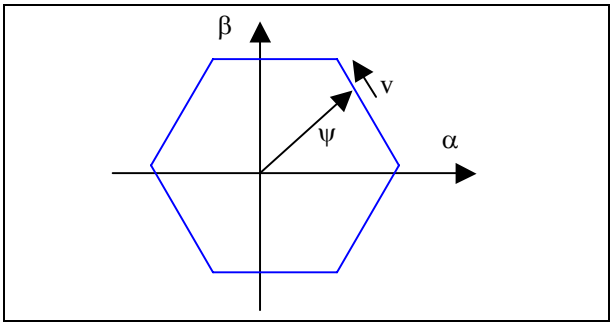

Figure 19. Displaced stator flux polygon

Other irregularities can cause the flux trajectory to become slightly flat or ellipsoid (causes $2 \cdot f_S$ at the DC side) or triangular (e. g., due to unsymmetrical snubber circuits, causes $3 \cdot f_S$).

Figure 20 below shows a measured example of the current components that are seen at the DC side of a 3-phase inverter during acceleration. Notice the switching pattern changes ("gearshifts") at t ≈ 45 s and t ≈ 50 s.

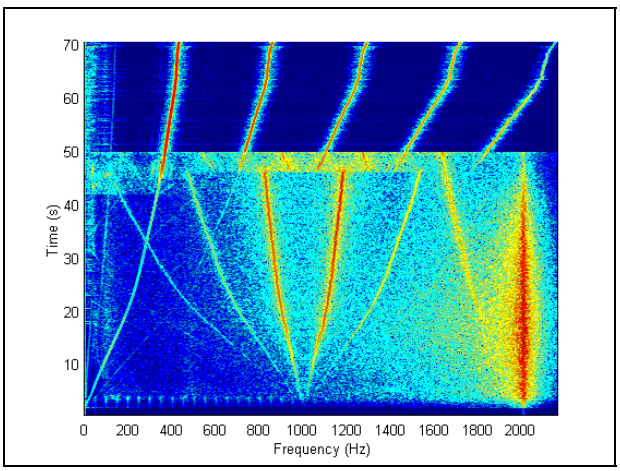

Figure 20. Inverter DC side current spectrum

Line filter design. The design of the line filter is governed by several requirements:

* The filter must be able to attenuate the harmonic currents generated by the 3-phase inverter to levels that are safe from an interference point of view, in particular at the carrier frequencies of the signalling systems

* The input impedance of the vehicle must be high enough such that the interference currents generated by external sources (if any) become acceptably low

* The dynamics of the closed loop control systems for the inverters and AC motors must be acceptable, i. e., enough energy must be stored in the DC link capacitor, and the time constant for current changes in the line inductor must be acceptably low

* Several infrastructure authorities have their own rules, such as "The input impedance must be inductive above xx Hz", or "The input impedance must be at least xx Ω at xx Hz"

Specification addendum # 3

* The RMS value of the 6th harmonic component in i_{DM} in the big motor / small inverter combination is approximately 200 A as f_S sweeps through the 60 Hz to 70 Hz band.

* The interference limit for Reed track circuits is 10 mA

Filter attenuation. The requirements above give that the filter must have a gain at 360 Hz of max. 50 μA/A. Neglecting resistances and assuming zero substation impedance, the gain of a normal L-C low-pass filter as shown in figure 15 is given by

$$\frac{i_L}{i_{DM}} = \frac{1}{1-\omega^2 LC} \qquad (must\ be \le 50\ \mu A/A)$$

Filter components. If a typical DC link capacitor value of 15 mF is used, this leads to a minimum inductance value of the line inductor of 260 mH. This is a completely unrealistic value, and other solutions must be considered, such as (combinations of) the following:

* A 4th order filter in a L-C-L-C configuration (as described in section 5, figure 38)

* Take the small motor - big inverter combination instead, with pulse pattern optimisation such that the 6th harmonic is minimized

* With the big motor - small inverter combination, corner folding could be used up to $f_S \ge 72$ Hz. This would reduce the inverter power by approximately 5 %

4. AC-AC TRACTION SYSTEMS: 4-QUADRANT LINE CONVERTER, MAIN TRANSFORMER, DC LINK, AND AC LINE FILTER

The 4-quadrant converter (4QC) converts the single-phase line voltage (15 kV 16 2/3 Hz or 25 kV 50 Hz) into a basically constant DC link voltage. This makes the 4QC very suitable in a back-to-back configuration with a 3-phase inverter for an asynchronous motor drive.

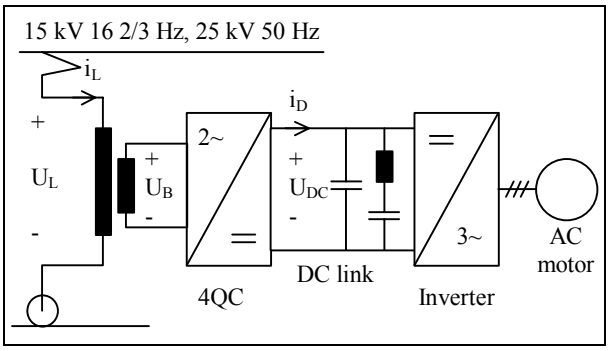

Figure 21. AC-AC traction system

In principle, the 4QC controls the power flow to the train by controlling the voltage drop across the short-circuit impedance of the main transformer [8]. Figure 22 shows the equivalent scheme of the line side circuits and the corresponding phasor diagram in motoring, with all quantities referred to the primary side.

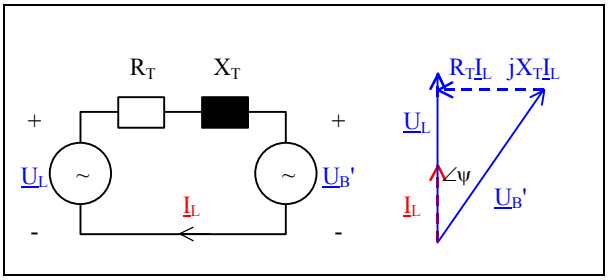

Figure 22. Equivalent scheme, line side circuits

The 4QC generates a voltage $\underline{U}_B'$ (' denotes reference to the primary side) with a variable fundamental amplitude and a variable phase angle ψ relative the line voltage $\underline{U}_L$. The current is determined by Ohms law:

$$\underline{I}_L = \frac{\underline{U}_L - \underline{U}'_B}{R_T + jX_T} \qquad \{11\}$$

It is normally desirable to adjust $\underline{U}_B'$ such that the reactive power is zero, i. e., cos(φ) = 1 in motoring as shown, and cos(φ) = -1 in regenerative braking.

Based on this, the main data of the line side circuits will now be calculated, i. e., the voltage ratio and short-circuit reactance of the main transformer, and the current rating of the 4QC. Given that a layout with 3 traction inverters was selected in section 1, the analysis will focus on a rather odd transformer with 3 secondary traction windings (i. e., one 4QC for each motor inverter).

Specification addendum # 4

* The DC link voltage at AC supply is 800 V.

* The auxiliary converters (for the 3·400 V and battery voltage supply on the train) are fed from the DC links, giving a total power including traction of 1500 kW.

* The system must be able to operate at full power at line voltages from 22 kV to 28 kV.

* The system must be able to operate at reduced power at line voltages up to 29 kV and down to 18 kV.

* The switching frequency of the 4QC is f_{SW} = 250 Hz per phase, and the minimum pulse time is t_{MIN} = 50 µs.

* The relative short-circuit transformer resistance is r_X = 2 %.

Transformer ratio. The transformer ratio tr is determined from the ratio between the highest required bridge voltage $|\underline{U}_B'|$ (referred to the primary), and the maximum voltage that can be generated by the 4QC from the DC link voltage (by PWM).

The required primary bridge voltage is calculated from the phasor diagram:

$$U'_{B,MAX} = \max\left\{ \frac{U_{L,MAX}}{\sqrt{\left(U_L - \frac{P}{U_L}R_T\right)^2 + \left(\frac{P}{U_L}X_T\right)^2}} \right. \qquad \{12\}$$

where U_L and P are varied within the actual limits for full operation. P is inserted with sign.
With the given parameters, the maximum 4QC bridge voltage is found as

$$U_{B,MAX} = \frac{(1 - f_{SW} \cdot t_{MIN}) \cdot U_{DC}}{\sqrt{2}} = 558\,V \qquad \{13\}$$

The transformer ratio tr is the result of {12} divided by the 558 V of {13}. This is shown in figure 23 below, vs. the relative short-circuit reactance of the transformer.

High transformer reactance values require a higher turn ratio. This is normally considered to be a disadvantage, because the secondary currents become higher at a given power level.

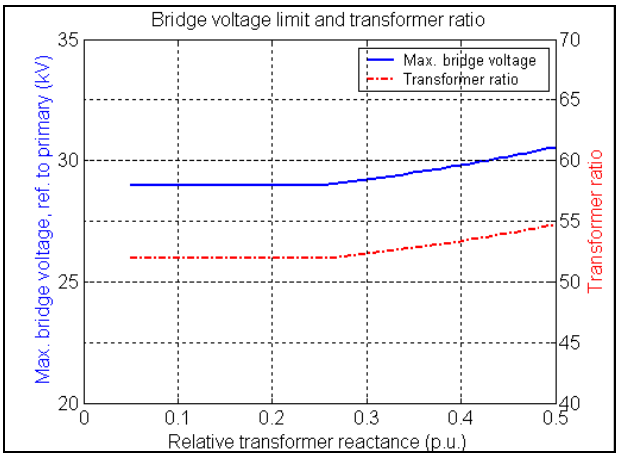

Figure 23. Max bridge voltage, transformer ratio.

2nd harmonic link. The current supplied to the DC link can be calculated by assuming the DC link voltage U_{DC} to be constant, and by neglecting the small power losses of the 4QC. The latter means that the power at the AC and DC sides must be equal:

$$\begin{aligned} p(t) &= \sqrt{2}U'_B\cos(\omega t-\psi)\cdot\sqrt{2}I_L\cos(\omega t) \\ &= U_{DC}i_D(t) \end{aligned} \qquad \{14\}$$

Carrying out the multiplications of the two cosine functions, and solving for $i_D(t)$ gives

$$i_D(t)=\frac{U'_B I_L}{U_{DC}}(\cos(\psi)+\cos(2\omega t-\psi)) \qquad \{15\}$$

The first term of {15} equals the active line power minus the power losses of the transformer, while the 2nd term expresses the normal double frequency power oscillation of a single phase AC system plus the reactive power consumed by the main transformer. It is customary to equip the DC link with a special filter branch tuned to the 2nd harmonic, in order to avoid excessive ripple voltages.

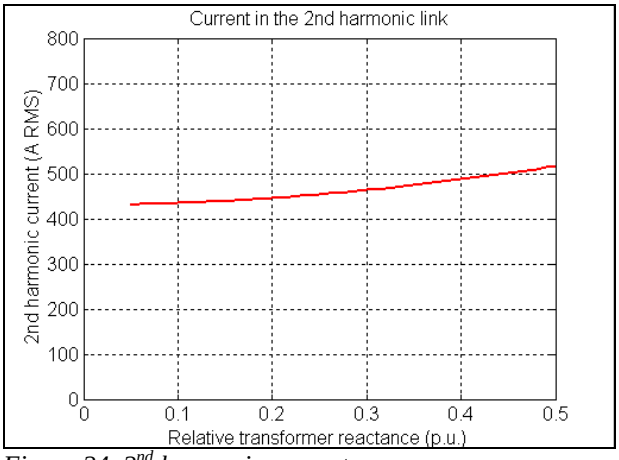

Figure 24. 2nd harmonic current

A voltage ripple across the DC link will lead to DC currents and torque pulsations in the traction motor when it operate with a stator frequency equal or close to the ripple frequency, unless the inverter is capable of compensating the ripple and deliver a symmetrical voltage wave shape. At 50 Hz line frequency, the inverter is typically operating in the full voltage mode according to figure 10, and an efficient compensation is hardly possible. This can put tight limits on the tolerances of the capacitor and inductor of the 2nd harmonic link.

4QC current capacity. The maximum RMS line current is found at maximum train power and minimum line voltage. Multiplying this current by the transformer ratio and dividing by the number of 4QCs (3 in this example) gives the maximum 4QC RMS current, shown by the solid curve in figure 25 below.

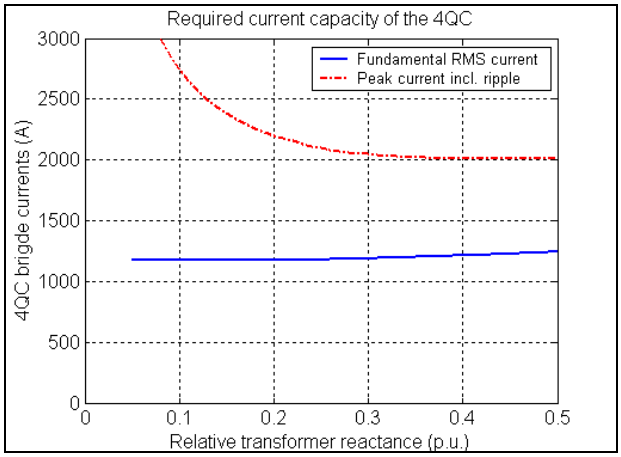

Figure 25. 4QC currents

However, from the point of view of semiconductor rating, the peak current is just as important as the RMS current. The highest instantaneous current is found when a notch in the 4QC PWM voltage pattern is located just at the peak of the current fundamental sinusoid. A voltage notch means that the 4QC short-circuits the transformer secondary winding, and the line voltage builds up the current.

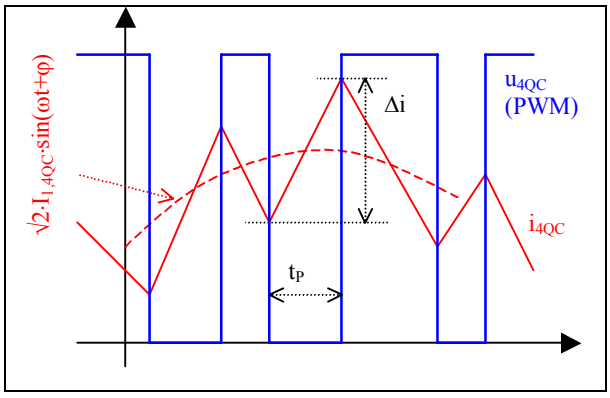

Figure 26. 4QC current ripple

The peak 4QC current is found as

$$\hat{i}_{4QC} = \sqrt{2} \cdot I_{1,4QC} + \frac{\Delta i}{2} \qquad \{16\}$$

with Δi approximately being calculated as

$$\Delta i = \frac{\pi\sqrt{2}(U_L - R_T I_L)(1 - \alpha \cdot \cos(\psi)) \cdot tr}{\frac{f_{SW}}{f_1} X_{T,W}} \qquad \{17\}$$

where $X_{T,W}$ is the transformer reactance per secondary winding, and α is the control ratio of the 4QC:

$$\alpha = \frac{\sqrt{2} \cdot U_{B,1}}{U_{DC}} \qquad \{18\}$$

The dash-dot line in figure 25 presents the calculated result with the actual set of parameters. In the typical case, this curve has a minimum at a relatively high transformer reactance value, meaning that the smallest converter size is obtained with a rather big transformer. It should be noted, however, that the technical development goes towards higher switching frequencies, meaning that the current ripple becomes less of an issue. Today, the 250 Hz used in this example is only seen in high-power locomotives.

4QC voltage spectrum. The 4QC bridge voltage is generated by means of PWM. The upper curves in figure 21 show the voltage references of the two phases of one 4QC (solid and dot-dash sinusoidals, respectively). The amplitude of these sinusoidals equals the modulation index α. The points of intersection with the triangular carrier (which has an amplitude = 1, and a frequency = f_{SW}) determines the switching instants as given by the phase potential references (middle curves). Finally, the lower curve shows the 4QC bridge voltage as the difference between the two-phase voltages.

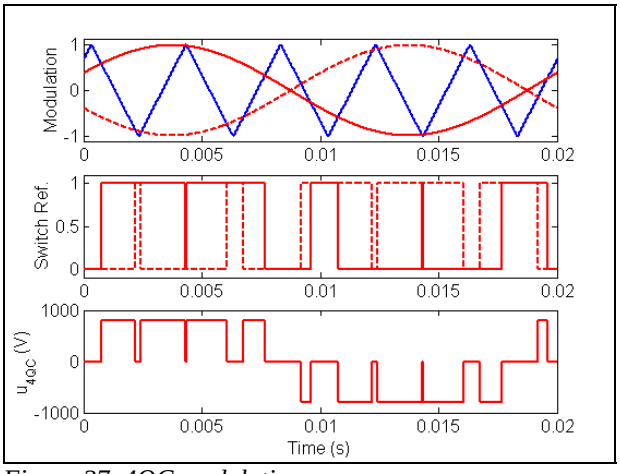

Figure 27. 4QC modulation

In addition to the 50 Hz fundamental, the (ideal) PWM pattern of one 4QC bridge produces a voltage spectrum with the main components located at the frequencies $n \cdot 2f_{SW} \pm k \cdot f_1$, with n = 1, 2, . . . and k = 1, 3, . . ., with the upper limit of k increasing as n increases.

When more 4QCs operate in parallel, with each unit connected to its own secondary winding on the transformer, it is common to interlace the switching, i. e., to introduce an appropriate phase shift between the triangular modulation carriers. This cancels the lower-order PWM harmonics, meaning that the main components of the interlaced spectrum are located at the frequencies $n_{4QC} \cdot n \cdot 2f_{SW} \pm k \cdot f_1$.

The harmonic spectrum (referred to the primary side) from the 3 interlaced 4QC bridges (n_{4QC} = 3) of the example is shown in figure 28. The levels of the individual odd harmonics vary with the control ratio α, such that the **O**'s indicate the levels seen at 25 kV and no load, while the *'s show the highest levels that are seen as the line voltage varies between 18 and 29 kV.

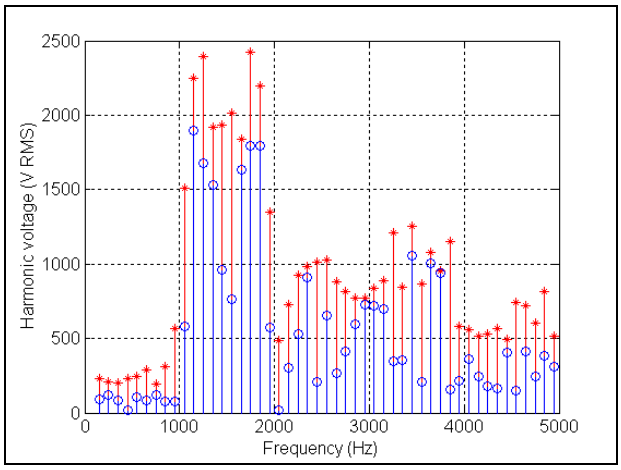

Figure 28. Bridge voltage spectrum, primary side

The main components of the spectrum are located around $n_{4QC} \cdot 2f_{SW}$ = 1500 Hz.

Line impedance characteristics. The calculation of the harmonic contents of the traction return current, e. g., in order to determine the psophometric current, must consider the impedance characteristics of the overhead supply line and return current system [9]. It is a common misunderstanding that a "conservative estimate" of the current harmonics can be made by assuming that the line impedance is 0. Actually, a line impedance of zero is far from worst-case.

The impedance of an overhead supply line (OHL) system is characterised by the following per unit length parameters:

* Series resistance	r	(Ω/m).
* Series inductance	l	(H/m)
* Capacitance to earth	c	(F/m)
* Conductance to earth	g	(1/Ωm)

Typically, r is frequency dependent r(ω), and at certain conditions, it might be necessary to include a frequency dependency of l as well.

The supply system for 50 Hz electrified railways is usually designed with a sectionised OHL. Each section is typically 10-40 km long with a substation at one end and a neutral section at the other. Seen from the neutral section (open end), the (complex) impedance $\underline{Z}_L$ of such a line is calculated as

$$\underline{Z}_L = \underline{Z}_C \cdot \frac{\underline{Z}_S + \underline{Z}_C \cdot \tanh(\underline{\gamma} \cdot l_L)}{\underline{Z}_C + \underline{Z}_S \cdot \tanh(\underline{\gamma} \cdot l_L)} \qquad \{19\}$$

with the characteristic impedance $\underline{Z}_C$

$$\underline{Z}_C = \sqrt{\frac{r(\omega) + j\omega l}{g + j\omega c}} \qquad \{20\}$$

the propagation constant $\underline{\gamma}$

$$\underline{\gamma} = \sqrt{(r(\omega) + j\omega l)(g + j\omega c)} \qquad \{21\}$$

the line length l_L, and the substation (or other termination) impedance $\underline{Z}_S$. If the OHL is fed from the substation transformer via cables, the impedance of these must be included in $\underline{Z}_S$.

Specification addendum # 5

* The line impedance parameters are r = 0.15 Ω/km, l = 1 mH/km, c = 15 nF/km, and g = 1 μ/Ωkm.
r(f) = r·(f/50)^0.5.

* The substation impedance is $\underline{Z}_S$ = 0.15 + jω·0.015 Ω.

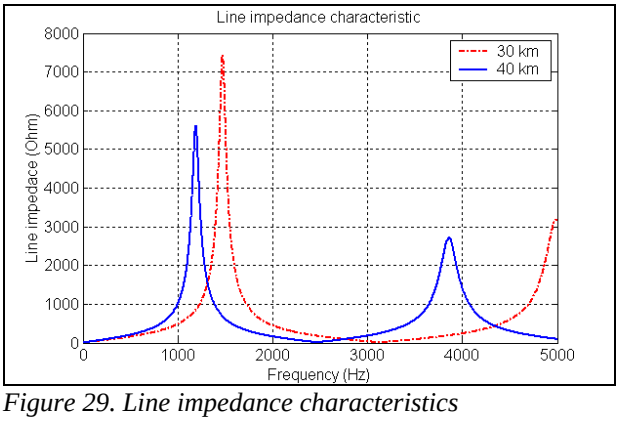

Figure 29. Line impedance characteristics

With these typical data, the calculated impedances seen from the far end of a 30 km and 40 km long line, respectively, are shown in figure 29. The impedance characteristics are subsequently inductive and capacitive, with parallel resonance at the peaks and series resonance at the minimums. Increasing the line length moves the resonance points downwards in frequency.

Figure 30, upper plot shows the impedance of the 40 km long line again, together with the input impedances of two different layouts of the actual train: One with a relative short-circuit reactance of 10 % (≈ 134 mH) and another with 40 % (≈ 535 mH), respectively.

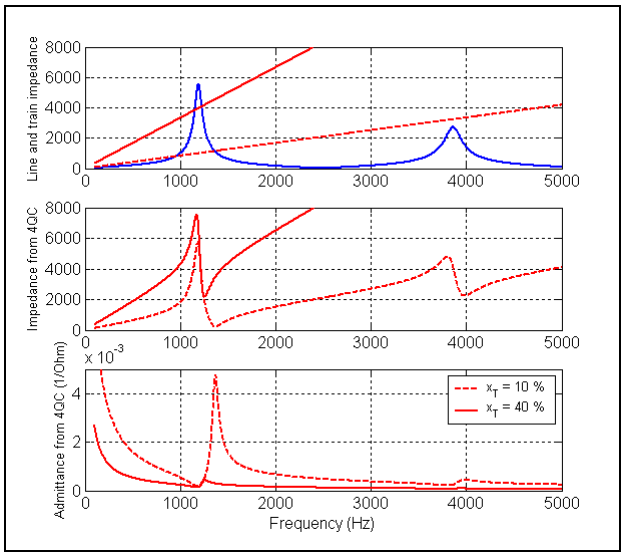

Figure 30. Line-vehicle resonance

The train and line impedance curves intersects each other in the 1 - 1.5 kHz band, where the line is capacitive (the impedance decreases with increasing frequency).

Seen from the 4QS, the capacitive line is connected in series with the inductive transformer, and the intersection of the curves is seen as a series resonance between these two impedances. The impedance of the series connection transformer + line is much lower with the lower transformer inductance, because the real part of the line impedance is much lower at this point. This is shown in the middle plot of figure 30.

The lower plot figure 30 shows that the peak admittance is 4.5 mA/V with the small transformer, but only 0.5m A/V with the bigger one.

4QC line current harmonics. Figure 28 showed that the RMS values of the 4QC voltage components (odd harmonics) in the example are approximately 2 kV in the 1 - 2 kHz band. If the peak of the admittance curve of figure 30 (lower) is located exactly at one of these odd harmonics, then the line current at this harmonic becomes very high: Approximately 9 A (4.5 mA/V

times 2 kV) with the 10 % transformer, and 1 A with the 40 % transformer.

This should be compared to the currents that would have been calculated if the line impedance had "conservatively" been assumed to be zero: Approximately 2.2 A and 0.55 A, respectively.

This leads to two important conclusions:

* The line harmonic interference can not be predicted without taking the line impedance into account

* The 4-fold increase in transformer inductance actually provides a 9-fold reduction of the harmonic interference currents

It is clear that the line-vehicle resonance will only be located exactly at a critical odd harmonic at certain specific line lengths. But given the number of different line feeding sections, and the number of parameters that can be varied within each feeding section (single or double track, normal or extended feeding, side tracks disconnected for maintenance, other vehicles on the line, etc.), the resonant condition will occur at some instant.

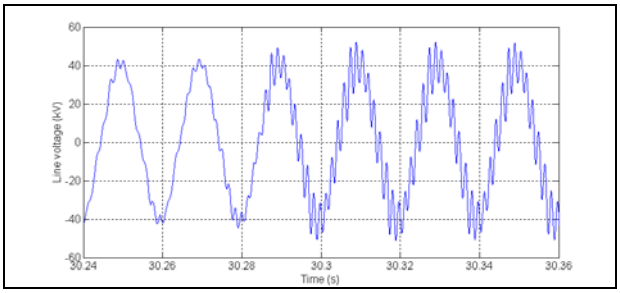

Figure 31. Measured line voltage at line-vehicle resonance conditions. The 4QCs are activated at t ≈ 30.28 s.

AC line filter. Another way of counteracting the line-vehicle resonance is by adding more resistance to the circuit. Seen from the pantograph, the two impedances (line and vehicle) are effectively connected in parallel, and the admittance peak corresponds to a parallel resonance between the two. The most efficient damping of a parallel resonance is provided by a shunt resistor. However, in order to minimise the losses at the 50 Hz fundamental, the resistor must be equipped with a series capacitor, and in some cases also with a shunt inductor. For practical reasons, such filters are normally connected to a dedicated, tertiary transformer winding, but in principle, such an arrangement is not different from a high voltage filter.

For simplified calculations, a T equivalent calculated from the standard short circuit impedances of the multiwinding transformer is sufficient.

In general, a full impedance matrix with all frequency dependent self and mutual impedances is required[1], and/or the T equivalent should be based on a set of measurements that exactly reflects the winding connections in actual operation.

Specification addendum # 6.

* The transformer has the following T equivalent: 25 % of the impedance to the primary, 75 % to the parallel secondary, and 0 to the filter.

* The filter is designed with a 350 Ω resistor in parallel with a 350 mH inductor, all of this in series with a 0.7 μF capacitor. All values referred to the primary side.

This gives the equivalent circuit shown in figure 32, which is valid for frequencies ≠ the fundamental.

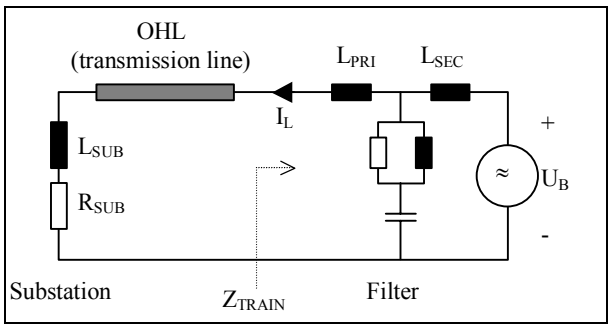

Figure 32. Equivalent circuit with AC line filter

The upper plot in figure 33 shows the new input impedances of the train including the filter, with x_T = 10 % and 40 %, respectively. Also the impedance of a 40 km line is shown as before.

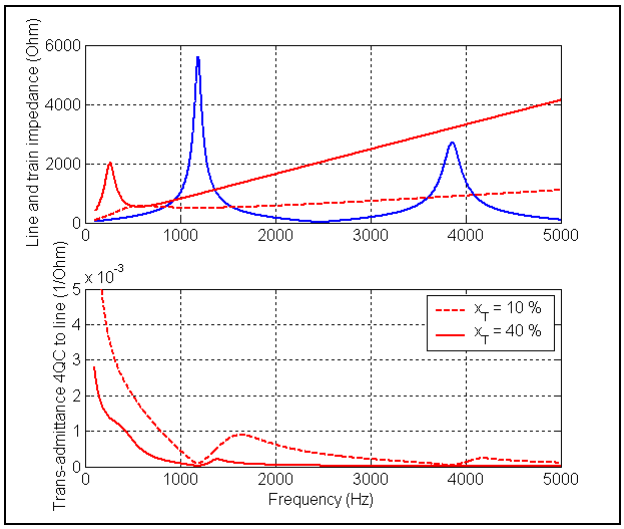

Figure 33. Line-vehicle interaction with AC line filter

[1] This is true in particular with the actual and non-typical transformer with 3 traction windings. There is no practical way such a transformer can be made with full symmetry.

The lower plot in figure 33 shows the transfer functions (or transadmittances) from 4QC voltage harmonics to line current harmonics (l_L = 40 km). In the critical 1 - 2 kHz band, these curves are considerably lower than the corresponding curves without a filter (figure 30).

Closed loop system stability. An AC line filter provides the further advantage that the stability margin of the 4QC control is improved [10]. The closed feedback loop of this control system comprises not only the vehicle itself, but also the overall electrical system outside the vehicle (supply system, other vehicles, etc.). Consequently, it is important to design the control systems in a robust fashion, and the design process must be supported by theoretical analysis.

A particularly adequate way of assessing the closed loop stability is given by the so-called input admittance criterion. An example is shown in figure 34 below.

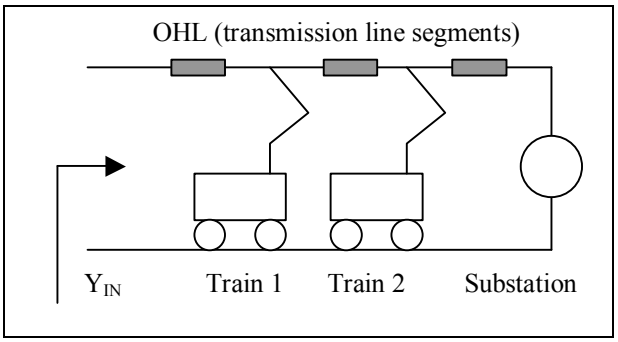

Figure 34. Stability analysis, input admittance criterion

The input admittance criterion says that if the imaginary part of the admittance $Im\{Y_{IN}\}$ seen at any point in the system is equal to zero at any frequency f_{RES} (this condition implies the existence of a resonance point), then the system is stable only if the real part of the input admittance $Re\{Y_{IN}\}$ is greater than zero at that frequency.

System stability can also be assessed by means of measurements [11], by using a locomotive as noise generator.

5. STEP-UP CHOPPERS FOR DC SUPPLY, AND HARMONIC INTERMODULATION

In some dual-system vehicles (25 kV AC and 750 V DC) such as the Class 92, the 4QCs are reconfigured at DC supply into step-up choppers that boost the 750 V DC line voltage to a DC link voltage of typically 1500 V DC. Other vehicles such as Class 375 are designed without a step-up chopper and operate with a DC link voltage equal to the line voltage. The following section will compare these designs to each other, and consider a number of typical problems in relation to EMI.

Figure 35. Class 92 dual system locomotive. *Photo by Mike Arm (arm@iname.com) [12]*

In the system without a step-up chopper (figure 36), DC power is fed directly to the inverter via a line inductor. The low-voltage side of the DC link is connected to earth in order to provide a return current path.

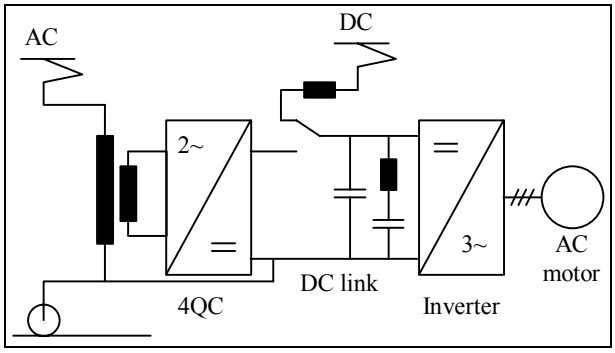

Figure 36. Dual voltage system, "direct on line"

In figure 37, each of the two 4QC phases make up a step-up chopper. Each chopper phase requires a phase inductor, meaning that an additional C-L line filter configuration is normally required.

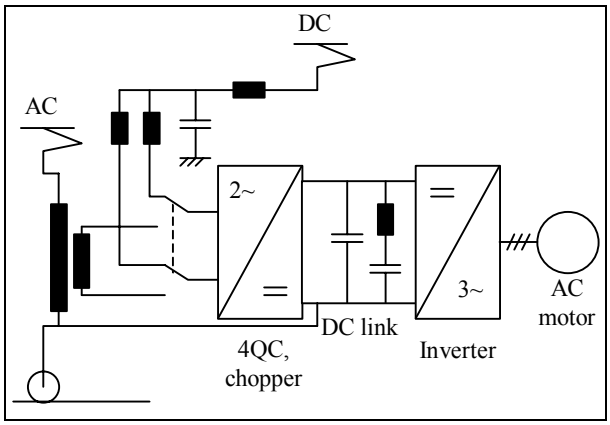

Figure 37. System using the 4QC as step-up choppers

EMI comparison. One of the arguments in favour of the system with step-up choppers is "better EMI performance", i. e., lower levels of line interference currents. The step-up chopper is claimed to provide a

barrier for the harmonic currents injected into the DC link by the 3-phase inverter.

A fair comparison must be made on an equal basis. So first, the 2nd order filter configuration in figure 36 is changed to a 4th order filter, like the one in figure 38.

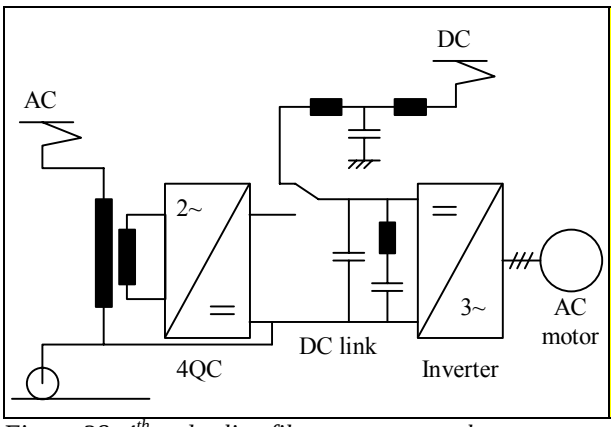

Figure 38. 4th order line filter, no step-up chopper

Now let all voltages, currents, and component values of the system without step-up chopper have the relative value 1, and let the DC link voltage of the step-up chopper solution be k (k > 1). This means that the choppers must have the control ratio $\alpha = 1/k$.

The step-up chopper is the equivalent of a transformer with the voltage ratio k. Assuming that the impedance of the DC supply is zero and that the harmonic currents injected into the DC link by the inverter are proportional to the motor currents, and by giving components in equal positions the same rated power, figure 39 provides a comparison.

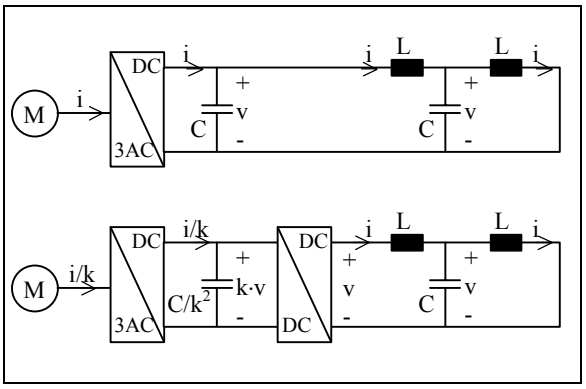

Figure 39. Comparison of currents and voltages

In the step-up chopper solution, the motor currents and thus the currents into the DC link are only 1/k'th of the levels in the system without step-up chopper. But due to the smaller capacitor (or more correctly, the lower capacitance, as the stored energy and thus the physical size of the capacitor is equal), this turns into a voltage ripple that is k times higher. With the voltage being reduced k times by the step-up chopper, the line currents become equal in the two systems.

Harmonic intermodulation. The upper plot in figure 32 shows the harmonic components of the chopper phase voltage at ideal conditions with a constant DC link voltage of 1875 V. With a DC line voltage of 750 V, this gives a chopper control ratio $\alpha = 0.4$, i. e., $k = 2.5$. The chopper frequency is f_C = 300 Hz, and the amplitude values of the voltage harmonics at n times f_C are found as

$$\hat{u}_n = U_{DC} \cdot \frac{2}{n\pi} \cdot \sin(n\alpha\pi) \qquad \{22\}$$

Values for n = 1, 2, and 3 are given in table 5. These levels are also found in figure 40, upper plot.

n	f	$\frac{2}{n\pi}\sin(n\alpha\pi)$	$\hat{u}_n$
1	300 Hz	0.605	1135 V
2	600 Hz	0.187	351 V
3	900 Hz	0.125	234 V

Table 5. Harmonic voltage amplitudes

In the middle plot, a 50 Hz component with an amplitude of $\hat{u}_R$ = 1875/2 = 937.5 V has been added to the DC link voltage. 50 Hz is a common signal system frequency. 937.5 V is obviously an unrealistic high value, selected only to make the plots visible.

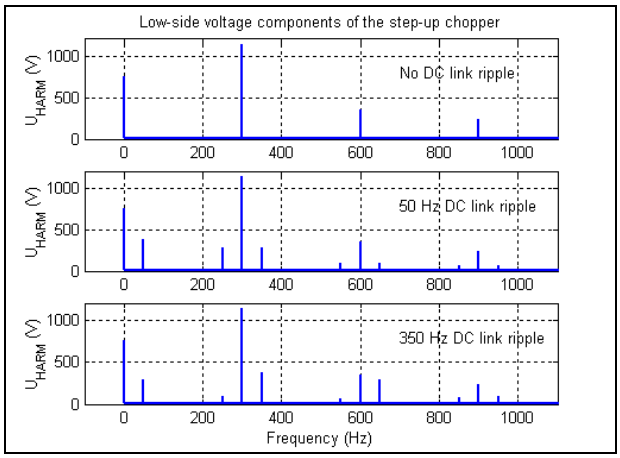

Figure 40. Chopper low-side voltage components

The 50 Hz component in the plot is $\alpha \cdot 937.5 = 375$ V as expected. But additional voltage harmonic components are seen as sidebands to $n \cdot f_C$, in 50 Hz distance. The amplitude of each sideband voltage component is:

$$\hat{u}_{s,n} = \hat{u}_R \cdot \frac{1}{n\pi} \cdot \sin(n\alpha\pi) \qquad \{23\}$$

In the lower plot, the frequency of the 937,5 V DC link ripple is 350 Hz, meaning that the sidebands now occur in 350 Hz distance from the chopper harmonics $n \cdot f_C$. I. e., with a step-up chopper running at f_C = 300 Hz, a 350 Hz component generated by the 3-phase inverter turns out to cause 50 Hz signal interference.

This harmonic intermodulation is generally undesirable, and restricts the overall system design in several ways. Consequently, step-up choppers should be restricted to cases where the required inverter power is so high that no semiconductors exist with a sufficient current rating. The Class 92 locomotive shown in figure 35 is an example of such a case.

Harmonic intermodulation in AC-AC traction. Harmonic intermodulation is also seen in AC-AC traction systems where any voltage ripple across the DC link is modulated by the fundamental frequency of the supply line. As an example, a 313 Hz DC link ripple voltage modulated by 50 Hz generates 363 Hz (as well as 263 Hz), and a 473 Hz ripple gives 423 Hz (and 523 Hz), meaning that the critical frequency band for reed track circuit interference caused by the 3-phase inverter is much wider than the reed band itself.

Other critical signalling frequencies at 50 Hz supply are 75 Hz and 125 Hz because interference components at these frequencies can be modulated forth and back between DC link voltage ripple and line current interference [10].

6. TESTING AND APPROVAL

The purpose of testing is 3-fold:

* The train manufacturer must convince himself that the train has been properly designed and built

* It must be demonstrated to the buyer of the train that all his performance requirements and other conditions have been met

* It must be demonstrated to the infrastructure owner and the relevant authorities that the train complies with all legal requirements, European and/or other standards, local interface specifications, etc.

The manufacturers own testing. Tests should be performed at several stages of a project:

* Component testing, e. g., 1000 h endurance testing of capacitors, or single-shot testing of semiconductors.

* Prototype testing, e. g., with a new inverter design using an inductive load in order to exactly define the operation points.

* Train control and communication system testing, i. e., running all computer-based systems against each other and (typically) against real time simulators.

* System testing with the complete traction system, using speed controlled motors as loads for the traction motors.

* Commissioning testing, i. e., the final testing of the first vehicle.

The following principles should apply to the testing:

* The test procedures and methods should not be specified by the person being responsible for the design himself, but by another person. The tests should not aim for demonstrating that everything has been done correctly, but with the purpose of finding the weak points, if any.

* The required amount of testing, and the complexity of the tests, increase at least in proportion to the technical complexity of the device under test.

Performance Testing. The performance of the vehicle used as example throughout this paper would typically be tested by loading it with sand bags to simulate maximum passenger load, and running it forth and back on the line. The run time between the two stations (or, in the general case, between any two stations as well as the complete line) is monitored, and it is checked that no components overheat after say 6 h of running according to the specified timetable.

The performance of a locomotive is typically tested at an acceleration test. A number of laden freight wagons corresponding to the maximum specified train weight are coupled after the locomotive, and this train is accelerated from standstill at the maximum specified gradient. The test is performed at different adhesion conditions (dry rail, wet rail, dry+sand, wet+sand, etc.), and relevant signals such as line voltage and current, drawbar force, speed, and distance, are recorded. Also continuous operation at maximum power for longer time must be part of the test program.

Figure 41. Tractive effort test, SNCB locomotive class 13 in Wasserbillig, Luxembourg. Photo by Paul Kettels, CFL

Other relevant performance tests could be the following:

* Winter tests (low temperatures, different types of snow, performance of the snow plough, etc.)

* Tunnel tests, i. e., testing for condensation of the air humidity at rapid changes of temperature (the so-called Simplon effect)

Figure 42. Winter tests, DB Cargo locomotives class BR185 and BR189 in Gällivare, Sweden, January 2003. Photo by Dietmar Aurich, Bombardier Transportation

Legal requirements, international standards, and local specifications. The split-up of the former national railway companies that has led to the present situation with at least 4 players in the game (the train manufacturer, the operator, the infrastructure owner, and the approving authority or inspectorate), has had a mushrooming effect on the acceptance procedures in most European countries. Even a brief discussion of this whole problem area could easily be the subject of several papers on their own, so here, only a few of the most important points will be listed:

* Each country is different, and all infrastructure owners and authorities have different requirements, traditions and expectations. It cannot be expected that experience from one country can be transferred to another.

* In general, the rules of the game are poorly specified. The interface specifications, if any, are faulty and incomplete, and the approval processes are not described at all or they are only described in general terms with a poor connection to the real world.

* The manufacturer must thoroughly consider the problems of vehicle acceptance already at the start of a new project, and develop comprehensive requirement specifications and approval procedures before any costly design work starts. In cooperation with the buyer of the vehicle, these documents should be discussed and agreed with the local infrastructure owner and authorities at an early stage. Basically, the manufacturer should always act as if the specifications he has received from his customer are incomplete, and seek his own additional information.

* No matter what else has been specified or not specified, certain requirements such as the European EMC Directive are mandatory within the EU.

* It is not customary to specify physical constants such as the gravitational acceleration $g \approx 9.82\ m/s^2$. This means, as an example, that the manufacturer must consider the transmission line behaviour of the OHL (section 4 above), even if the line impedance parameters have not been explicitly specified. The manufacturer must accept that he is expected to have a high level of technical competence, and that it is his own responsibility to maintain and develop this competence through journals, magazines, etc., and through adequate training and education of his personnel.

Figure 43. Interference Tests, Class 357 "Electrostar" EMU in Cerhenice, Czech Republic. Photo by Peter Mellberg, Bombardier Transportation

References

1. Filipović Ž,1991,
"Elektrische Bahnen", Springer Verlag, Berlin, DE

2. Östlund S, and Leksell M, 1992,
"Elektrisk Traktionsteknik", KtH Stockholm, SE

3. Fischer R, 1986,
"Elektrische Maschinen", Carl Hanser Verlag, München, DE

4. Teich W, 1972,
"Dieselelektrische Triebfahrzeuge mit schleifringlosen Asynchronfahrmotoren", Elektrische Bahnen 43 (1972) 4, 74-88

5. Lege B and Thoma C, 2000,
"Viersystemlokomotive Baureihe 189 für DB Cargo", Elektrische Bahnen 98 (2000) 8, 298-299

6. Depenbrock M, 1985,
"Direkte Selbstregelung (DSR) für hochdynamische Drehfeldantriebe mit Stromrichterspeisung", etz-Archiv 7 (1985), Heft 7, 211-218

7. Takahashi I and Noguchi T, 1986,
"A New Quick-Response and High-Efficiency Control Strategy of an Induction Motor", IEEE Transactions on Industry Applications, Vol. IA-22, No. 5, 9/10 (1986)

8. Kehrmann H, Lienau W, Nill R, 1974,
"Vierquadrantensteller - eine netzfreundliche Einspeisung für Triebfahrzeuge mit Drehstromantrieb", Elektrische Bahnen 45 (1974), 135-142

9. Holtz J, Klein H-J, 1989,
"The Propagation of Harmonic Currents Generated by Inverter-Fed Locomotives in the Distributed Overhead Supply System", IEEE Transactions on Power Electronics, Vol. 4, No. 2, April 1989, 168-174

10. Buhrkall L, 1999,
"AC-AC Traction", http://www.buhrkall.dk

11. Lörtscher M, Meyer M, Hemmer B, Schneeberger A, 2001,
"Kompatibilitätsuntersuchungen am schweizerischen 16.7-Hz-Bahnstromnetz", Elektrische Bahnen 99 H 6-7 (2001), 292-300

12. Photo copied from The European Railway Picture Gallery, http://mercurio.iet.unipi.it/pix/pix.html

Abbreviations and Symbols

a	Acceleration
α	Modulation index, control ratio
B	Braking effort, magnetic flux density
c	Capacitance per unit length
Δ	Delta, e. g.: Δs: small distance
η	Efficiency
F	Force, tractive effort
f	Frequency
φ, ϕ	(Phase) Angle
G	Gradient
g	Gravitational acceleration ≈ 9.82 m/s^2, conductance per unit length
γ	Wave propagation constant
I, i	Current
J	Surface current density
j	Imaginary unit = $\sqrt{-1}$
k	Constant
l	Length, inductance per unit length
m	Mass
μ	Friction coefficient
n	Integer number
ω	Rotational speed, angular frequency
P, p	Power
ψ	(Phase) Angle
R	Resistance
r	Resistance per unit length
s	Distance
T	Torque
t	Time
U, u	Voltage
V	Volume
v	Velocity, speed
X	Reactance
Z	Impedance

Address of the author:

Lars Buhrkall
Sviegade 3
DK - 6760 Ribe

Tel. +45 74 84 60 11
Fax +45 74 84 60 33
GSM +45 24 40 76 97
Email lars@buhrkall.dk
www.buhrkall.dk